Model for the line shapes of complex ions in hot and dense plasmas

A. Calisti, F. Khelfaoui, R. Stamm, and B. Talin
Physique des Interactions Ioniques et Moléculaires, Université de Provence, Centre de St. Jérôme, 13397 Marseille, France

R. W. Lee
University of California, Lawrence Livermore National Laboratory, Livermore, California 94550
(Received 12 March 1990)

A model for calculating the profile of spectral lines emitted by multielectron emitters in a hot plasma is described. The Stark broadening is included in the model by using the static ion approximation and an impact approximation for the electrons. The atomic data required for the line-shape calculation are extracted from an atomic structure code and prepared as data necessary for the excited and ground levels of the radiative transition. For the cases where electron broadening is much smaller than the average ionic Stark shift, an approximation is proposed to obtain rapidly a diagonal form of the evolution operator for the emitter. Line shapes of lithiumlike and berylliumlike ions have been calculated under the conditions of recent experiments performed in laser-produced plasmas.

I. INTRODUCTION

The study of the line shapes emitted by multielectron ions has recently focused the interest of several groups.[1-3] These studies have been motivated largely by experimental advances which use the observation of line shapes of complex ions in plasmas studied for inertial confinement fusion (ICF), or for x-ray laser development. Moreover, the need for an accurate treatment of the line shapes that are used in opacity models for the study of the transport of radiation through stellar interiors has also been recently emphasized.[4] A decisive factor in the development of theoretical studies of complex ion line shapes is the continuing improvement of computing facilities, allowing the generation and handling of large amounts of atomic data for use in line broadening formalisms.

Three main mechanisms affect the broadening of the emission lines of complex ions. The Doppler broadening produced by the thermal motion of the radiating ions is generally the dominant mechanism in a low-density plasma with emitters having a moderate core charge z. For increasing z values, spontaneous emission is enhanced roughly as z^4, and natural broadening may well exceed Doppler broadening. For higher plasma densities, the plasma microfield generally broadens the line through the Stark effect, and Stark broadening may then govern the line shape. This paper describes a line-shape formalism designed to calculate the line profile of an arbitrary atomic structure, in a plasma with a large range of conditions. The corresponding computer code accepts atomic data from a standard atomic structure code. The line profile of a multielectron emitter is calculated for a selected spectral range, in the presence of natural broadening and Doppler and Stark effects.

The model used for the description of the Stark effect assumes that the plasma and atomic structure parameters are such that the static ion microfield approximation and the model of a binary collision electronic operator are valid. On the one hand, an electronic collision operator can usually safely be used, however, on the other hand, neglecting ion motion requires that the width of the line is much larger than the typical fluctuation frequency of the ion microfield. Since the breakdown of the static approximation has been found to occur for hydrogenic emitters in ICF plasma conditions,[5,6] a careful check for the validity of this approximation has thus to be done for each line in hot and dense plasma conditions. In our static ion model, an average is performed over a static microfield distribution obtained by the adjustable parameter exponential approximation (APEX) method,[7] which allows rapid and accurate calculations.

In the following, we present in Sec. II the formalism and describe the principal numerical techniques used in the model. A technique based on the diagonalization of the emitter's evolution operator for a set of sampled ion microfields is described. This technique allows a drastic reduction in the computer time required to obtain the line shape of a complex atomic structure. The connection of the line-shape formalism with the atomic data found in a standard atomic structure code is discussed in Sec. III. Examples of studies are given and discussed in Sec. IV.

II. LINE-SHAPE FORMALISM

The usual starting point for a line-shape formalism is given by the dipole autocorrelation function expressed as a trace over the emitter states:[8]

$$C(t)=\mathrm{Tr}[\mathbf{d}T^{\dagger}(t)\mathbf{d}T(t)\rho_0]_{\mathrm{av}} \tag{1}$$

where $\mathbf{d}$ and T are the dipole and evolution operator of the emitter, and ρ_0 is the density matrix for the emitter only. Owing to the weak coupling between the emitter

and the perturbers, it has been assumed that the initial density matrix can be factorized in an emitter and perturber term. The average in Eq. (1) has to be taken over all plasma perturber states. We define two subsets, a and b, of states and denote their states respectively by $\alpha,\alpha',\cdots$ and $\beta,\beta',\cdots$. Assuming that the perturbers do not induce transitions between subsets a and b, and disregarding the density matrix,[9] we may write $C(t)$ as the sum

$$C(t)=\sum_{\alpha,\beta,\alpha',\beta'}[\langle\alpha|\mathbf{d}|\beta\rangle\langle\beta|T^{\dagger}(t)|\beta'\rangle \times\langle\beta'|\mathbf{d}|\alpha'\rangle\langle\alpha'|T(t)|\alpha\rangle]_{\mathrm{av}} . \quad (2)$$

This expression can be written in a compact form by using a Liouville space formalism:[8,10]

$$C(t)=\langle\langle\mathbf{d}^{\dagger}|[U]_{\mathrm{av}}|\mathbf{d}\rangle\rangle . \quad (3)$$

The emitter evolution operator U in Liouville space is defined by

$$\langle\langle\alpha\beta|U|\alpha'\beta'\rangle\rangle=\langle\alpha'|T|\alpha\rangle\langle\beta|T^{\dagger}|\beta'\rangle . \quad (4)$$

Double bra and ket vectors are defined as usual in Liouville space. The average over the plasma perturbers in Eqs. (2) and (3) is performed in two steps. The electron component is assumed to interact with the emitter through binary collisions. The whole effect of the electrons may then be represented by an electronic collision operator of the type described in the Appendix. This electronic collision operator constitutes the main part of the homogeneous broadening mechanism. A second step consists of an average over the ions screened by the electrons. This average over the ions, together with the Doppler broadening, constitute the inhomogeneous part of the broadening. The quasistatic ion approximation which has been used leads to an average over a microfield distribution function $w(q)$. A method for the calculation of a microfield distribution valid for all conditions from weakly to strongly coupled plasmas[7] has been chosen.

Our model leads to the following form of the evolution operator U_q, averaged over the electrons in a constant ion field q:

$$U_q(t)=e^{-i(L_q-i\Phi)t} \quad (5)$$

where L_q is the Liouville operator of the quantum system of interest, perturbed by a static external electric field q. The diagonal elements of this operator are atomic frequencies, and the nondiagonal terms, the Stark interaction terms. The non-Hermitian diagonal operator Φ represents all the homogeneous broadening effects, i.e., the electronic and natural broadening.

It is now possible to write the correlation function $C(t)$ as

$$C(t)=\int w(q)S_q(t)dq \quad (6)$$

where S_q is defined as

$$S_q(t)=\langle\langle\mathbf{d}^{\dagger}|U_q(t)|\mathbf{d}\rangle\rangle . \quad (7)$$

The spectral intensity of the emitted radiation is proportional to the Laplace transform of S_q averaged over microfield states:

$$I(\omega)=\frac{1}{\pi}\mathrm{Re}\left[\int w(q)\int_0^{\infty}e^{i\omega t}S_q(t)dt\,dq\right] . \quad (8)$$

The line shape results from a competition between inhomogeneous and homogeneous broadening. Due to degeneracy removal, the Stark effect breaks each initial line into many Stark components on which natural and electronic relaxation act as a noise filter. This suggests the possibility of replacing the integral for the microfield average with a weighted sum over n_q terms:

$$I(\omega)=\sum_{q=1}^{n_q}W_qI_q(\omega) . \quad (9)$$

In this expression $I_q(\omega)$ is the line-shape function for a fixed ion field with label q, and the data set W_q is chosen in order to optimize computer time and accuracy for the final line profile.

At this point there are two paths which can be followed: Either we perform the Fourier transform and then invert the resulting matrix, or we explicitly express $e^{-i(L_q-i\Phi)t}$ and Fourier transform it. The latter path is preferred because it generally leads to large reductions in computer time.

In order to follow this path, the basic idea is to look for the basis in which $L_q-i\Phi$ is diagonal. In such a basis, let us denote by $|k\gg$ the eigenvectors of $L_q-i\Phi$, with complex eigenvalues $z_k=x_k+iy_k$. If M_q is the similarity transformation matrix, we may write the line-shape function in an electric microfield strength q by

$$I_q(\omega)=\frac{1}{\pi}\mathrm{Re}\left\langle\left\langle\mathbf{d}^{\dagger}\left|M_q\int_0^{\infty}e^{i\omega t}e^{-iM_q^{-1}(L_q-i\Phi)M_qt}M_q^{-1}dt\right|\mathbf{d}\right\rangle\right\rangle . \quad (10)$$

The Fourier transform in this expression is easily performed, leading to the following structure for I_q:

$$I_q(\omega)=-\frac{1}{\pi}\mathrm{Im}\left\langle\left\langle\mathbf{d}^{\dagger}\left|M_q\begin{pmatrix}\frac{1}{\omega-z_1} & & \\ & \ddots & \\ & & \frac{1}{\omega-z_n}\end{pmatrix}M_q^{-1}\right|\mathbf{d}\right\rangle\right\rangle \quad (11)$$

This expression can be written as

$$I_q(\omega)=\sum_k\frac{\beta_k(\omega-x_k)+\alpha_ky_k}{(\omega-x_k)^2+y_k^2} \quad (12)$$

where the sum is over the eigenvalues of $L_q-i\Phi$, and the coefficients α_k and β_k depend on the values of the operators $\mathbf{d}$ and M_q. The expression in Eq. (11) for $I_q(\omega)$ shows that the coefficients α_k and β_k can be calculated separately for each eigenvalue.

A very useful approximation can be used to simplify all the previous expressions and further reduce the computer time. L_q is a real and symmetric matrix which is diago-

nalized more easily than $L_q - i\Phi$. For a real symmetric matrix, an orthogonal similarity transformation M_q exists such that $L_q' = M_q^T L_q M_q$ is diagonal with M_q real and $M_q^T = M_q^{-1}$ (M_q^T is the matrix transposed of M_q). For the conditions where homogeneous broadening is small compared to the broadening produced by the static ions, it is indeed possible to diagonalize the Liouville operator alone, and express the evolution operator as

$$U_q = M_q e^{-i(L_q' - i\Phi')t} M_q^T \tag{13}$$

where Φ' is the diagonal part of the homogeneous broadening operator written in the base diagonalizing L_q:

$$\Phi_{ij}' = (M_q^T \Phi M_q)_{ij} \delta_{ij} . \tag{14}$$

The condition for the validity of this approximation is that the elements of Φ' are smaller than those of L_q. This condition is well satisfied if the average Stark splitting (given by the nondiagonal elements of L_q), is much larger than the homogeneous width. We have performed tests to evaluate the error made by using this approximation. For cases where the average Stark splitting is larger by an order of magnitude than the homogeneous width, the difference between profiles calculated with a diagonalization of $L_q - i\Phi$, and profiles obtained with this approximation, is within the numerical uncertainties (less than 1%). On the other hand, for the cases where the average Stark splitting is much smaller than the homogeneous width, the operator $L_q - i\Phi$ is essentially diagonal, thus requiring no calculation. Significant errors have been found only for cases where the average Stark splitting is of the order of the homogeneous width. Discrepancies are generally found in the dip between two components, whereas the widths and maximum intensities of the components always agree to better than 20%. For the profiles reported below, the difference between the two calculations was always smaller than 5% throughout the profiles.

III. CONNECTION WITH ATOMIC DATA

The calculation of the line profile requires knowledge of the ionic energy levels and their associated quantum numbers. This calculation also supposes that quantities like the Liouville, dipole, and homogeneous broadening operators are connected to the data available in a standard atomic structure code. The spectra shown in Sec. IV have been obtained by using the atomic data calculated by a multiconfiguration Dirac-Fock code developed by Grant *et al.*[11]

In the following, we shall distinguish between states, levels, and configurations, and respectively note these as $|\gamma,J,M\rangle$, $|\gamma,J\rangle$, and $|\gamma\rangle$. The first step in our model consists of selecting subsets of levels within an atomic database. All the levels involved in radiative transitions whose frequencies belong to a chosen spectral range are selected. In addition all levels linked to those levels involved in the radiative transitions by an allowed transition are also selected. This procedure results in two subsets of levels, *a* and *b*: Among the levels of subset *a* are all the initial levels, and among the levels of subset *b* are all the final levels of the radiative transitions. Obviously, the larger the selected level subsets, the larger the matrices involved in the evolution operator. In practical applications, other criteria may be applied in order to reduce the quantum systems to a tractable size on a given computer.[12]

The minimum information required for each chosen level to calculate the line profile associated with a given system will be a label, the energy, the quantum number J, and the spontaneous-emission damping rate; and for each transition, the lower and upper label of the two connected levels and the oscillator strength.

The Liouville matrix elements are calculated according to

$$L = \frac{1}{\hbar}(H \otimes I^d - I \otimes H^d) . \tag{15}$$

In this equation superscript d means dual space operator.

As mentioned above, we denote by $\alpha,\alpha',\alpha'', \cdots$ and $\beta,\beta',\beta'', \cdots$ the states in subsets *a* and *b*. The distinction between radiative dipoles associated with the

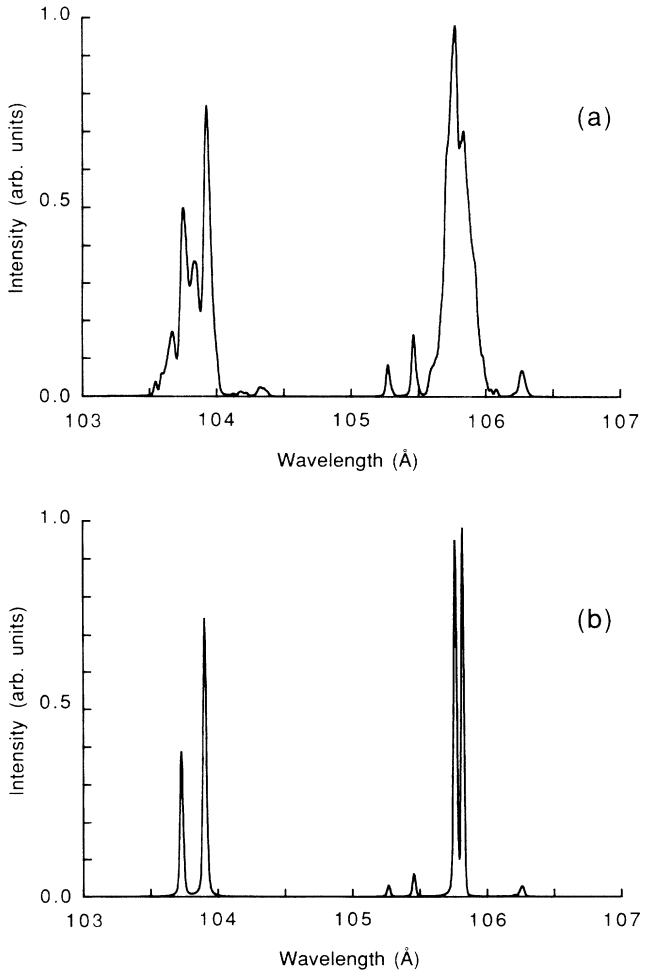

FIG. 1. Lithiumlike aluminum spectrum of the $n=5$ to 3 transition, for a density $N_e = 3.3 \times 10^{19}$ cm^{-3} and a temperature $T = 200$ eV. The ion microfield is taken into account in (a), and neglected in (b).

$\langle\beta|\mathbf{d}|\alpha\rangle$ matrix elements and Stark dipoles associated with the $\langle\beta|\mathbf{d}|\beta'\rangle$ or $\langle\alpha|\mathbf{d}|\alpha'\rangle$ terms is introduced. Note that, due to the no quenching approximation (no Stark $\langle\beta|\mathbf{d}|\alpha\rangle$ terms), $U_q(t)$ is block diagonal. Therefore this also results in a substantial reduction of computational time.

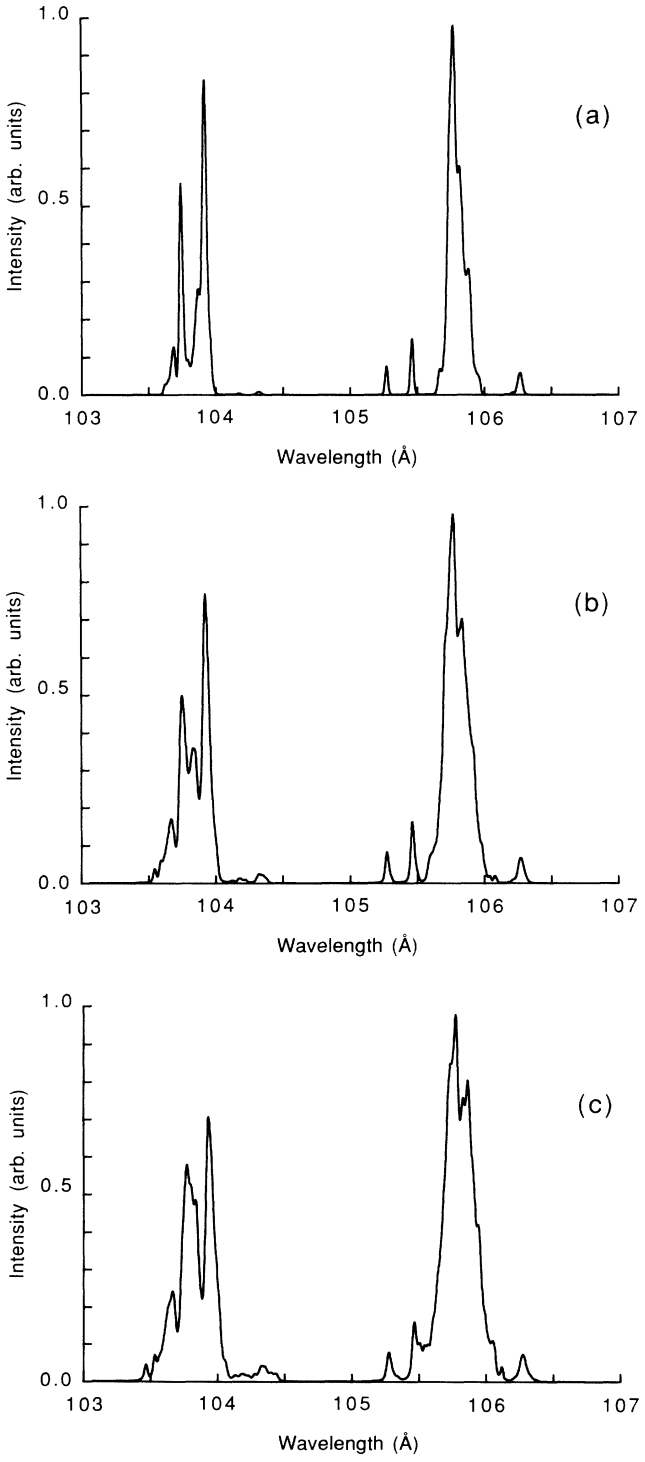

FIG. 2. Lithiumlike aluminum spectrum of the $n=5$ to 3 transition, for a temperature $T=200$ eV, and the electronic densities (a) $N_e=10^{19}$ cm^{-3}, (b) $N_e=3.3\times10^{19}$ cm^{-3}, (c) $N_e=6\times10^{19}$ cm^{-3}.

In the Liouville subspace, generated with the $|\alpha\beta\rangle\rangle$ basis, the matrix elements of the real symmetric operator L_q are

$$\begin{aligned}&\langle\langle\alpha\beta|L_q|\alpha\beta\rangle\rangle=\omega_{\alpha\beta}\ ,\\&\langle\langle\alpha\beta|L_q|\alpha\beta'\rangle\rangle=\langle\beta|d|\beta'\rangle q\ ,\\&\langle\langle\alpha\beta|L_q|\alpha'\beta\rangle\rangle=-\langle\alpha|d|\alpha'\rangle q\ ,\end{aligned}\tag{16}$$

where q is the local static electric field, and $\omega_{\alpha\beta}$ is the energy of the radiative transition from state α to state β.

Using the Wigner-Eckart theorem, the electric dipole matrix elements are related to the reduced dipole matrix element $\langle\gamma J\|\underline{P}^{(1)}\|\gamma' J'\rangle$ by the relation[13]

$$\langle\gamma JM|d_\mu|\gamma' J'M'\rangle=(-1)^{J-M}\begin{pmatrix}J & 1 & J'\\ -M & \mu & M'\end{pmatrix}\times\langle\gamma J\|\underline{P}^{(1)}\|\gamma' J'\rangle\ .\tag{17}$$

In the 3-j symbol, $\mu=0,\pm1$ corresponds to the three spherical tensor components d_z and $d^{\pm}=\mp(1/\sqrt{2})(d_x\pm id_y)$ of the electric dipole. The reduced dipole matrix elements are related to the dipole line strength S, and to the oscillator strength f_{ji} between a state of the upper level j to all the states of the lower level i by[13]

$$S=|\langle\gamma J\|\underline{P}^{(1)}\|\gamma' J'\rangle|^2\tag{18}$$

and

$$f_{ji}=\frac{E_i-E_j}{3(2J'+1)}S\ .\tag{19}$$

For highly charged emitters, spontaneous emission may contribute to the linewidth because the transition probability strongly increases with the emitter charge. Denoting by λ (in centimeters) the wavelength of the transition from an upper state $|\gamma' J'M'\rangle$ to a lower level $|\gamma J\rangle$, the transition probability is[13]

$$A=\frac{2.0261\times10^{-6}}{2J'+1}S\left[\frac{1}{\lambda}\right]^3\ \text{sec}^{-1}\ .\tag{20}$$

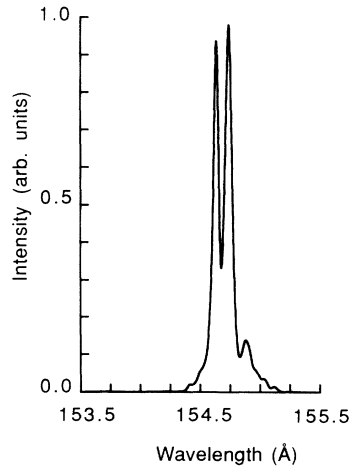

FIG. 3. Lithiumlike aluminum spectrum of the $4f$-$3d$ line, for a density $N_e=3.3\times10^{19}$ cm^{-3} and a temperature $T=200$ eV.

The total spontaneous-emission rate for a given state results from a sum over all lower levels. As already pointed out, this natural broadening is accounted for in the formalism with a coefficient Γ added to the diagonal elements of the electron collision operator:

$$\Gamma=\tfrac{1}{2}(A_i+A_j) \tag{21}$$

where A_i and A_j are the total spontaneous-emission rates of the initial and final state of the transition.

Finally, the atomic database is used to evaluate the electronic collision operator because this operator contains the scalar product $\mathbf{d}\cdot\mathbf{d}$. Neglecting the interference term between the initial and final subsets of states restricts the calculation of $\mathbf{d}\cdot\mathbf{d}$ only to these two subsets of states. Such approximations can be removed in a straightforward manner, but it is kept in the present work to make the numerical application of this model simple. For the numerical applications here the $\mathbf{d}\cdot\mathbf{d}$ term has been calculated by extracting the atomic data for the selected subsets of states. The complete form of the electronic collision operator is given in the Appendix.

IV. EXAMPLES OF STUDIES

Various experimental studies have been performed on lithiumlike aluminum lines[14–16] in a recombining laser-produced plasma. In particular the $4f$-$3d$ and $5f$-$3d$ lines have been shown to exhibit population inversion and gain. Using our model, we have performed several line-shape calculations for these lines using the plasma conditions of the experiment of Moreno *et al.*[16] In this experiment, the linewidth of the $5f$-$3d$ line was measured to be 0.35 Å, which greatly exceeds the Doppler and instrumental widths. A theoretical evaluation by Moreno *et al.* indicates that Stark broadening is responsible for the increased width of the $5f$-$3d$ line.

We have used our model to calculate a detailed line shape including Stark and Doppler broadening for the $n=5$ to 3 transition. The corresponding spectrum is plotted in Fig. 1(a) in the wavelength range between 103 and 107 Å for a density $N_e=3.3\times10^{19}$ cm^{-3} and a temperature $T=200$ eV. The $n=5$ to 3 transition has two main features which correspond roughly to the broadened $5d$-$3p$ line (between 103.5 and 104.5 Å), and $5f$-$3d$ (between 105.5 and 106 Å) lines. Smaller components surrounding the latter line correspond to $5s$-$3p$ and $5p$-$3d$ lines. The role of Stark effect due to the ionic microfield is exemplified by comparing this profile to the profile of Fig. 1(b) which has been obtained in the absence of ionic microfield. The latter profile, which corresponds to electron and Doppler broadening only, yields linewidths which are smaller by about an order of magnitude than those of Fig. 1(a).

A good qualitative agreement of our calculation in Fig. 1(a) has been found with the result of the measurements by Moreno *et al.*[16] In particular, it is possible to identify the strongest Stark broadened spectral features and to demonstrate a reasonable agreement between their observed and our predicted line profile. Precise agreement is not expected because the measured profiles correspond to population inversion conditions, whereas our calculations are performed assuming local thermodynamic equilibrium. The linewidth of the calculated $5f$-$3d$ line is 0.22 Å, which is about 40% smaller than the measured width.[16] Although likely to be small for these plasma conditions, the inclusion of ion dynamic effects[6] in our model would further increase the linewidth. Further experimental effects such as instrument resolution, gradients in the plasma, and turbulence will also increase the line width.

A set of three profiles of the $n=5$ to 3 transition is plotted in Fig. 2 for a temperature $T=200$ eV in order to demonstrate the role of the Stark effect as the density is increased from 10^{19} to 6×10^{19} cm^{-3}. Over this density range, the components of the $n=5$ to 3 transition are seen to be simultaneously split and broadened by the Stark effect.

Similar observations can be made for the $n=4$ to 3 transition, as, for example, in the case of the $4f$-$3d$ (154.7 Å) line plotted in Fig. 3. A reasonable overall agreement is found between the line shape of our calculation and the experiment of Moreno *et al.*[16]

It is well known that if the plasma microfield causes shifts comparable with the energy level splittings, the wave functions of the neighboring states become mixed, thus allowing the observation of transitions which would be forbidden in the absence of microfield. An example is provided in Fig. 3 by the forbidden $4d$-$3d$ (154.9 Å) component which is predicted by our calculation to appear on the red side of the $4f$-$3d$ (154.7 Å) line. An inspection of the experimental profile of Ref. 16 reveals that a line is observed at about 154.9 Å, but the intensity ratio of this line to the allowed line is larger by a factor 2.5 than is predicted by our model. In order to further investigate the reason for this discrepancy, we have calculated with our model the $4f$-$3d$ line for several densities between 3.3×10^{19} cm^{-3} and 3.3×10^{20} cm^{-3}. The intensity ratio of the forbidden to allowed line is increased in this density domain by a factor 2.2, thus still remaining 20% smaller than the experimental value for $N_e=3.3\times10^{20}$ cm^{-3}, the largest density case calculated. The temperature has been found to only weakly affect this line ratio. Indeed, a temperature decrease by a factor of 2 decreases the line ratio by about 20%. All this suggests that the experimental uncertainties in the determination of the density and temperature cannot alone explain the difference between the measured and calculated line ratio. Possible explanations for this difference could be either related to the time integration of the measurements[16] or to the existence of a density gradient effect. A similar comparison is not possible in the case of the $n=5$ to 3 transition, because the large linewidth prevents the observation of the forbidden lines.

Woltz and Hooper[2] have recently performed calculations of lithiumlike and berylliumlike krypton lines and compared their results to spectra obtained from laser implosion experiments for densities, N_e between 10^{23} and 10^{24} cm^{-3}. Fairly good agreement between the experiment and the calculated profiles of Ref. 2 has been found in the general shape and position of the principal spectral features. In order to compare to the results of Ref. 2, we have used our model to calculate the Li-like $n=4$ to 2

transition for four different densities at a temperature of $T=1100$ eV. The resulting Stark and Doppler spectra plotted in Fig. 4 confirm the previously observed behavior of the line as the density is increased. In the calculated density range, the Stark effect gradually broadens and splits the two components of the two main spectral features. Note that the inclusion of instrumental broadening in our calculations would bring the profiles of Fig. 4 into close agreement with the results of Ref. 2. Some differences remain, however, the most conspicuous being that the homogeneous broadening is estimated to be about 30% larger in our calculations than in those of Ref. 2. Such a difference is not surprising, however, because a different model, based on the use of Coulomb wave functions, has been used to evaluate the electron broadening operator of Ref. 2. The difficulties of an accurate calculation of the electron broadening in the case of multielectron ions have been discussed in Ref. 3. These difficulties have been recently exemplified by a comparison of experimental and theoretical results in the case of the isolated (thus unaffected by the quasistatic ion microfield) $3s$-$3p$ line of Li-like C IV, N V, and O VI.[17] The theoretical results reported in Ref. 17 generally predict electron widths which are smaller but within 40% of the observed values. Compared to the experimental values of Ref. 17, the electron broadening operator used in our model has been found to be slightly larger (by 10% for C IV and 6% for N V) or in good agreement (for O VI). This shows that, for these three particular emitters, our model provides at least the same degree of agreement with the experiment as the other theoretical approaches. It is suggested in Ref. 17 that a better agreement would require a more precise calculation of the strong collision contributions to the electronic broadening. Future work will concern the inclusion of electronic quadrupole contribution in our model.

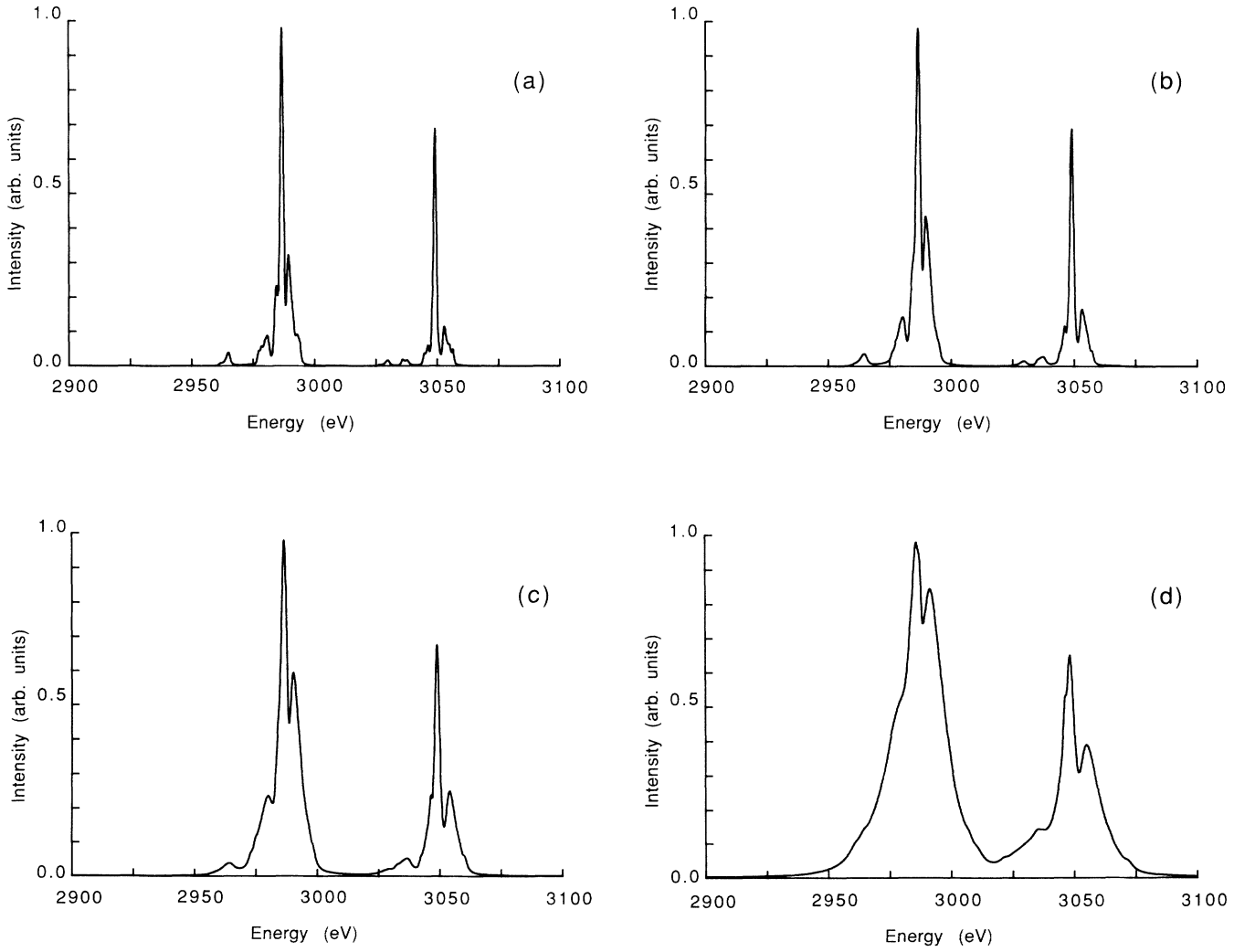

FIG. 4. Lithiumlike krypton spectrum of the $n=4$ to 2 transition, for a temperature $T=1100$ eV and the electronic densities: (a) $N_e=10^{23}$ cm^{-3}, (b) $N_e=2\times10^{23}$ cm^{-3}, (c) $N_e=4\times10^{23}$ cm^{-3}, and (d) $N_e=10^{24}$ cm^{-3}.

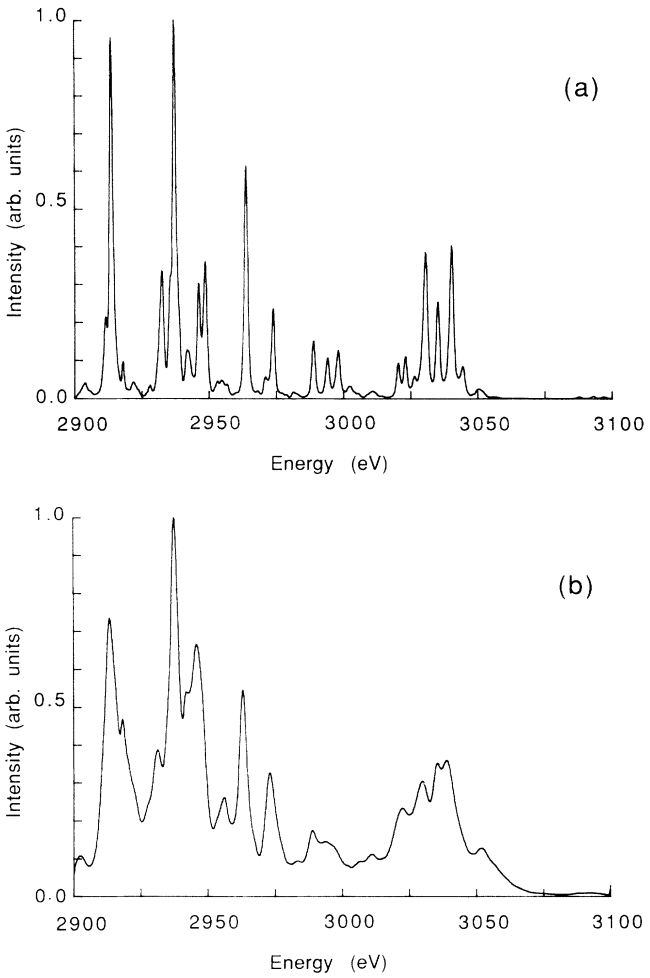

FIG. 5. Berylliumlike krypton spectrum of the $n=4$ to 2 transition, for a temperature $T=1100$ eV and the electronic densities (a) $N_e=1.5\times10^{23}$ cm^{-3} and (b) $N_e=10^{24}$ cm^{-3}.

Similar conclusions may be drawn more readily from the case of the $n=4$ to 2 transition of Be-like krypton plotted in Fig. 5, than from the preceding Li-like calculations. For a temperature $T=1100$ eV, the Be-like krypton line shape is barely affected by the Stark effect for $N_e=1.5\times10^{23}$ cm^{-3}, whereas the Stark effect is the dominant broadening mechanism for $N_e=10^{24}$ cm^{-3}. The inclusion of instrumental broadening would also bring our Be-like profile in close agreement with the calculations of Ref. 2.

V. CONCLUSION

We have described a model for the calculation of line shapes emitted by multielectron ions in a hot and dense plasma. The basic approximations used are identical to those found in standard line broadening formalisms. A nonstandard approximation may optionally be used to rapidly diagonalize the emitter evolution operator in case the homogeneous operator is smaller than the static ionic broadening. A computer code based on this model has been developed with a careful choice of rapid numerical techniques. This has allowed the study of a variety of cases on a desk-top computer, the Digital Equipment Corporation Microvax II. For laser-plasma conditions, the profiles calculated with our model have been shown to be strongly modified by the Stark effect due to the ionic microfield. Our calculations of the $n=5$ to 3 and $n=4$ to 3 transitions of lithiumlike aluminum demonstrate the role of the ionic Stark effect for the $5f$-$3d$ line, confirming previous estimates.[16] Our calculated line profiles are in good agreement with recently calculated and measured profiles[2] of lithiumlike and berylliumlike krypton lines in laser implosion conditions. For these plasma conditions, our results confirm the role of the Stark effect previously described in Ref. 2. These results also demonstrate that standard line-shape models using accurate atomic data provide reliable spectra which may be used as a plasma diagnostic for emitters with complex atomic structures.

ACKNOWLEDGMENTS

This work has been supported in part by the University of California, Lawrence Livermore National Laboratory under Contract No. 1061503. The Physique des Interactions Ioniques et Moléculaires is "Unité associée au Centre National de la Recherche Scientifique No. 773."

APPENDIX

The electronic collision operator represents the effect of the electronic microfield component on the radiator. It is usually calculated in the framework of a binary collision relaxation theory. An element of this collision operator may be written as the sum of three terms[18]

$$\phi_{\alpha\alpha'\beta\beta'}=\sum_{\alpha''}\delta_{\beta\beta'}\mathbf{d}_{\alpha\alpha''}\cdot\mathbf{d}_{\alpha''\alpha'}G(\Delta\omega_{\alpha''\beta})+\sum_{\beta''}\delta_{\alpha\alpha'}\mathbf{d}_{\beta'\beta''}\cdot\mathbf{d}_{\beta''\beta}G(-\Delta\omega_{\alpha\beta''})-\mathbf{d}_{\alpha\alpha'}\cdot\mathbf{d}_{\beta'\beta}[G(\Delta\omega_{\alpha\beta'})+G(-\Delta\omega_{\alpha'\beta})]\ . \quad \text{(A1)}$$

In this expression we have used $\Delta\omega_{\alpha\beta}=\omega-\omega_{\alpha\beta}$. The two first terms are sums over perturbing states α'' and β'', and the last term represents the interference effect between the subsets a and b. The function $G(\omega)$ depends on the density and temperature of the plasma and is calculated to second order in the radiator-electron interaction. A thermal average included in $G(\omega)$ may be performed by using a quantum-mechanical relaxation theory[2] or a classical path assumption[3] for the perturbing electrons. The line shapes shown in this paper have been calculated with an expression for $G(\omega)$ based on a modified semiclassical model, in which a strong-collision term C is added to the semiclassical term.[19] For nondegenerate systems, the integrand of the thermal average contains oscillating exponentials of the frequency difference $\omega_{\alpha\alpha''}$ between the state α and perturbing states α''. We have tried to model this behavior by introducing in the thermal average an impact parameter cutoff at $b=v/\omega_{\alpha\alpha''}$. The quantity $G(\omega)$ may thus be written

$$G(\omega)=-\frac{4\pi}{3}\left[\frac{2m}{\pi kT}\right]^{1/2}N_e\left[\frac{\hbar}{me}\right]^2\left[C+\int_y^\infty e^{-x}\frac{1}{x}dx\right] \quad \text{(A2)}$$

where y is given by

$$y=\left[\frac{\hbar n^2}{2z}\right]^2\frac{\omega^2+\omega_p^2+\omega_{\alpha\alpha''}^2}{E_{\mathrm{H}}kT}\ . \tag{A3}$$

In this expression, n is the principal quantum number of state α, z is the charge of the ionic core, ω_p is the plasma frequency, and E_{H} the ionization energy of hydrogen. In the calculations of Sec. IV, the interference term in Eq. (A1) has been omitted and the impact limit expression $G(\omega=0)$ has been taken. The latter approximation will only affect the wing of the lines for values of ω of the order or larger than v/ρ_W (ρ_W being the Weisskopf radius). Finally, only the diagonal elements of Φ have been retained for the calculations of Sec. IV, since the nondiagonal terms have been found to be negligible for these cases.

[1]M. J. Seaton, J. Phys. B **20**, 6363 (1987).
[2]L. A. Woltz and C. F. Hooper, Jr., Phys. Rev. **38**, 4766 (1988).
[3]H. R. Griem, in *Spectral Line Shapes,* edited by J. Szudy (Ossolineum, Warszawa, 1989), Vol. 5, p. 17.
[4]C. A. Iglesias, F. J. Rogers, and B. G. Wilson, Astrophys. J. Lett. **322**, L45 (1987).
[5]R. Stamm, Y. Botzanowski, V. P. Kaftandjian, B. Talin, and E. W. Smith, Phys. Rev. Lett. **52**, 2217 (1984); **54**, 2170 (1985).
[6]R. Stamm, B. Talin, E. L. Pollock, and C. A. Iglesias, Phys. Rev. A **34**, 4144 (1986).
[7]C. A. Iglesias, J. L. Lebowitz, and D. MacGowen, Phys. Rev. A **28**, 1667 (1983).
[8]M. Baranger, in *Atomic and Molecular Processes,* edited by D. R. Bates (Academic, New York, 1964), Chap. 13.
[9]H. R. Griem, *Spectral Line Broadening by Plasmas* (Academic, New York, 1974).
[10]U. Fano, Phys. Rev. **131**, 259 (1963).
[11]I. P. Grant, B. J. McKenzie, P. H. Norrington, D. F. Mayers, and N. C. Pyper, Comput. Phys. Commun. **21**, 207 (1980).
[12]A. Calisti, F. Khelfaoui, R. Stamm, L. Sylvander, and B. Talin, Université de Provence report, 1989 (unpublished).
[13]R. D. Cowan, *Theory of Atomic Structure and Spectra* (University of California Press, Berkeley, 1981).
[14]P. Jaegle, G. Jamelot, A. Carillon, and C. Wehenkel, Jpn. J. Appl. Phys. **17**, 483 (1978).
[15]P. Jaegle, G. Jamelot, A. Carillon, A. Klisnick, A. Sureau, and H. Guennou, J. Opt. Soc. Am. B **4**, 563 (1987).
[16]J. C. Moreno, H. R. Griem, S. Goldsmith, and J. Knauer, Phys. Rev. A **39**, 6033 (1989).
[17]F. Böttcher, P. Breger, J. D. Hey, and H. J. Kunze, Phys. Rev. A **38**, 2690 (1988).
[18]E. W. Smith and C. F. Hooper, Jr., Phys. Rev. **157**, 126 (1967).
[19]H. R. Griem, M. Blaha, and P. C. Kepple, Phys. Rev. A **19**, 2421 (1979).